



# Enzyme Architecture: Remarkably Similar Transition States for Triosephosphate Isomerase-Catalyzed Reactions of the Whole Substrate and the Substrate in Pieces

Xiang Zhai, Tina L. Amyes, and John P. Richard\*

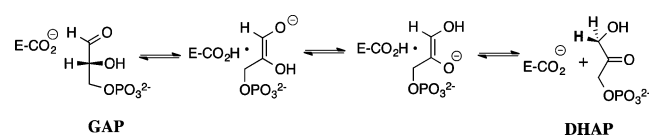
Department of Chemistry, University at Buffalo, State University of New York, Buffalo, New York 14260, United States

## Supporting Information

**ABSTRACT:** Values of  $(k_{\text{cat}}/K_{\text{m}})_{\text{GAP}}$  for triosephosphate isomerase-catalyzed reactions of (R)-glyceraldehyde 3-phosphate and  $k_{\text{cat}}/K_{\text{HPi}}K_{\text{GA}}$  for reactions of the substrate pieces glycolaldehyde and  $\text{HPO}_3^{2-}$  have been determined for wild-type and the following TIM mutants: I172V, I172A, L232A, and P168A (TIM from *Trypanosoma brucei*); a 208-TGAG for 208-YGG loop 7 replacement mutant (L7RM, TIM from chicken muscle); and, Y208T, Y208S, Y208A, Y208F and S211A (yeast TIM). A superb linear logarithmic correlation, with slope of  $1.04 \pm 0.03$ , is observed between the kinetic parameters for wild-type and most mutant enzymes, with positive deviations for L232A and L7RM. The unit slope shows that most mutations result in an identical change in the activation barriers for the catalyzed reactions of whole substrate and substrate pieces, so that the two transition states are stabilized by similar interactions with the protein catalyst. This is consistent with a role for dianions as active spectators, which hold TIM in a catalytically active caged form.

Triosephosphate isomerase (TIM) catalyzes the stereospecific and reversible conversion of dihydroxyacetone phosphate (DHAP) to (R)-glyceraldehyde 3-phosphate (GAP), by a proton transfer mechanism through enzyme-bound *cis*-enediolate intermediates (Scheme 1).<sup>1–4</sup> The 12 kcal/mol

Scheme 1



stabilization of the transition state by interactions between TIM and the remote phosphodianion group of substrate accounts for ~80% of total transition-state stabilization.<sup>5</sup> These binding interactions not only anchor substrate to the enzyme active site but also play a role in activating TIM for deprotonation of bound carbon acid, as shown by the large effect of the deletion of a phosphodianion gripper loop on  $k_{\text{cat}}$  for TIM-catalyzed isomerization of GAP<sup>6</sup> and by the large activation by exogenous phosphite dianion ( $\text{HPi}$ ) of TIM-catalyzed deprotonation of glycolaldehyde (GA)<sup>7</sup> and isomerization of  $[1\text{-}^{13}\text{C}]$ -glycolaldehyde ( $[1\text{-}^{13}\text{C}]$ -GA) to  $[2\text{-}^{13}\text{C}]$ -GA.<sup>8</sup> This utilization of the

binding energy of the nonreacting phosphodianion in enzyme activation, observed here and for other enzymatic reactions,<sup>7,9–13</sup> is a critical difference between reactions catalyzed by enzymes<sup>14,15</sup> and catalysis by small molecules.<sup>16</sup>

We report here a linear free-energy relationship, with slope of 1.0, between the kinetic parameters for the reactions of GAP and the pieces GA and  $\text{HPi}$  catalyzed by wild-type and structural mutants of TIM. This correlation shows that the transition states for the two reactions are stabilized by similar interactions with the protein catalyst and that the reactions proceed through similar transition states.

The I172 V,<sup>17</sup> I172A,<sup>17,18</sup> and P168A<sup>19,20</sup> mutants of TIM from *Trypanosoma brucei* (*Tbb*TIM) and the 208-TGAG for 208-YGG loop 7 replacement mutant (L7RM)<sup>19,21</sup> of TIM from chicken muscle (*c*TIM) were examined in earlier work. The Y208T, Y208S, Y208A, Y208F, and S211A mutants of yeast TIM (*y*TIM) were prepared, purified, and characterized as described in the Supporting Information (SI). The positions of these amino acid residues are shown in Figure 1, for the complex between DHAP and TIM from yeast.<sup>22</sup> The kinetic parameters determined for the Y208F and S211A enzyme-catalyzed

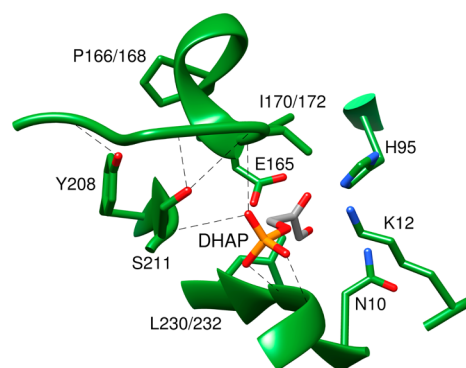


**Figure 1.** A model, from an X-ray crystal structure, of the complex between TIM from yeast and DHAP (PDB entry 1NEY) showing the amino acids mutated in this work. The side chains of H95, K12, and N10 play key roles in catalysis of the isomerization reaction.<sup>2,3</sup> Small differences in the numbering of the amino acids at TIM from the different sources used in these studies are noted, where appropriate: (*c*TIM or *y*TIM and *Tbb*TIM): Pro 166 and 168, I170 and 172, L230 and 232.

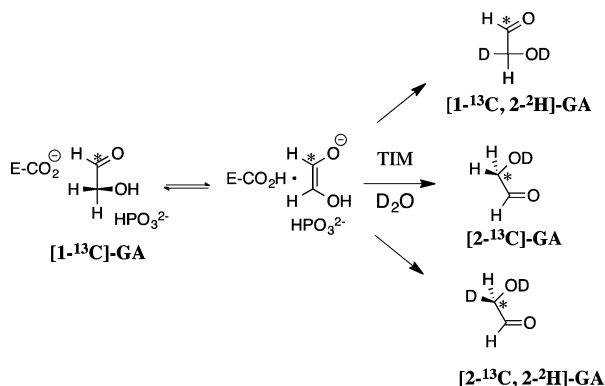
Received: January 31, 2014

Published: March 3, 2014

isomerization of GAP are in good agreement with the published values of Sampson and Knowles.<sup>23</sup>

The second-order rate constants ( $k_{\text{cat}}/K_{\text{m}}$ )<sub>obs</sub> for TIM-catalyzed reactions of [1-<sup>13</sup>C]-GA in D<sub>2</sub>O and the fractional yields, ( $f_{\text{p}}$ )<sub>E</sub>, of products [2-<sup>13</sup>C]-GA, [2-<sup>13</sup>C, 2-<sup>2</sup>H]-GA, and [1-<sup>13</sup>C, 2-<sup>2</sup>H]-GA (Scheme 2) were determined by monitoring

Scheme 2



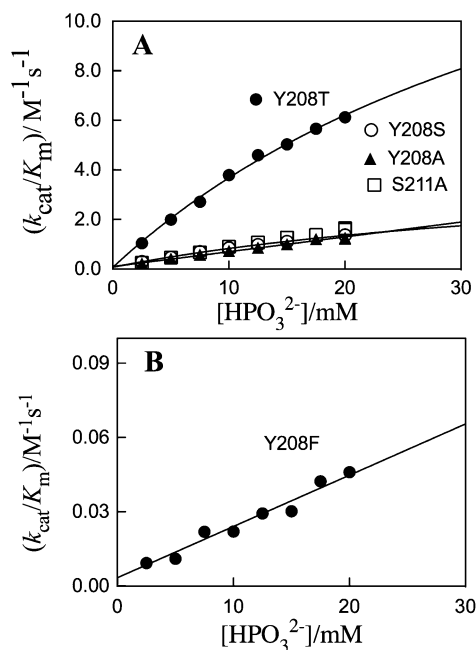
the disappearance of [1-<sup>13</sup>C]-GA and the formation of products by <sup>1</sup>H NMR.<sup>8</sup> Tables S1–S6 report kinetic and product data for the reactions catalyzed by wild-type  $\gamma$ TIM and by the Y208T, Y208S, Y208A, Y208F, and S211A mutant enzymes. A significant yield of [1-<sup>13</sup>C, 2,2-di-<sup>2</sup>H]-GA is sometimes observed from the TIM-catalyzed reactions of [1-<sup>13</sup>C]-GA,<sup>8,17,19</sup> where the dideuterium-labeled product is formed by a nonspecific protein-catalyzed reaction.<sup>8,24,25</sup> This is a minor product (5–10% yield) of the Y208T, Y208S Y208A, S211A mutant enzyme-catalyzed reactions of [1-<sup>13</sup>C]-GA in the presence of HP<sub>i</sub> and the major product (30–40% yield) of the reactions catalyzed by the severely crippled Y208F mutant. When the total yield of [2-<sup>13</sup>C]-GA, [2-<sup>13</sup>C, 2-<sup>2</sup>H]-GA and [1-<sup>13</sup>C, 2-<sup>2</sup>H]-GA [ $\sum(f_{\text{p}})_{\text{E}}$ , eq 1] is less than quantitative, the second-order rate constants ( $k_{\text{cat}}/K_{\text{m}}$ ) for reactions at the enzyme active site (Scheme 2) were determined from the observed second-order rate constant ( $k_{\text{cat}}/K_{\text{m}}$ )<sub>obs</sub> and the sum of the yields of the three products [ $\sum(f_{\text{p}})_{\text{E}}$ ], using eq 1.<sup>17,19</sup>

$$\frac{k_{\text{cat}}}{K_{\text{m}}} = \left[ \frac{k_{\text{cat}}}{K_{\text{m}}} \right]_{\text{obs}} \sum (f_{\text{p}})_{\text{E}} \quad (1)$$

Figure 1 shows the active site for a complex between  $\gamma$ TIM and DHAP.<sup>22</sup> I172 and L232 from *Tbb*TIM function in a hydrophobic clamp.<sup>26</sup> The basicity of the side chain of E167, which reacts to deprotonate the carbon acid substrate, is enhanced by interactions with the side chain of I172.<sup>27</sup> Steric interactions between the side chains of P168 and loop 7, induced by the ligand-gated conformational change,<sup>1,2</sup> force the E167 (*Tbb* numbering) carboxylate toward the carbon acid substrate.<sup>20,28</sup> This conformational change is enabled by formation of hydrogen bonds between the side-chain hydroxyls of Y208 and S211 from loop 7, respectively, with the backbone amide nitrogen of A176 and G173 from loop 6 and a hydrogen bond between the carbonyl oxygen of A169 and the  $\gamma$ -O of S211. The I172 V,<sup>17</sup> I172A,<sup>17</sup> L232A,<sup>17,18</sup> and P168A<sup>19,20</sup> mutations of *Tbb*TIM, the 208-TGAG for 208-YGGGS loop 7 replacement mutation (L7RM) of *c*TIM,<sup>19,21</sup> and the Y208 and S211 mutations of  $\gamma$ TIM each modify the enzyme structure in the region of the active site. Most of these structural mutations result

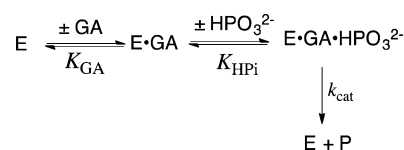
in a decrease in the kinetic parameters for the TIM-catalyzed reactions of whole substrates and substrate pieces. This reflects the destabilization of the respective transition states for the mutant enzyme-catalyzed reactions, which result from subtle effects of these mutations on enzyme structure.

Figure 2 shows the dependence on [HPO<sub>3</sub><sup>2-</sup>] of  $k_{\text{cat}}/K_{\text{m}}$  for the reactions of [1-<sup>13</sup>C]-GA catalyzed by Y208 and S211 mutants



**Figure 2.** Dependence of  $k_{\text{cat}}/K_{\text{m}}$  for the TIM-catalyzed turnover of the free carbonyl form of [1-<sup>13</sup>C]-GA in D<sub>2</sub>O on [HPO<sub>3</sub><sup>2-</sup>] at pD 7.0, 25 °C, and an ionic strength of 0.10 (NaCl). (A) Reactions catalyzed by the Y208T, Y208S, Y208A, and S211A mutants of  $\gamma$ TIM. (B) Reactions catalyzed by the Y208F mutant.

Scheme 3



of TIM. The third-order rate constants  $k_{\text{cat}}/K_{\text{GA}}K_{\text{HP}_i}$  (Scheme 3) reported in Table S7 were determined as the slopes of linear plots of  $k_{\text{cat}}/K_{\text{m}}$  against [HPO<sub>3</sub><sup>2-</sup>] for the reactions catalyzed by the Y208F, Y208A, and S211A mutants or as the slopes of the linear portions of the plots of data at low [HPO<sub>3</sub><sup>2-</sup>] for the reactions catalyzed by Y208S and Y208T mutants. Table S7 also reports the kinetic parameters  $k_{\text{cat}}$  and ( $k_{\text{cat}}/K_{\text{m}}$ )<sub>GAP</sub> for wild-type and mutant TIM-catalyzed isomerization of GAP.

The activation barrier for conversion of TIM and GAP to the transition state for enzyme-catalyzed isomerization of GAP [ $\Delta G_{\text{GAP}}^{\ddagger}$ ] is defined by the second-order rate constant ( $k_{\text{cat}}/K_{\text{m}})_{\text{GAP}}$ , while the barrier to formation of the transition state for the TIM-catalyzed reaction of the substrate pieces GA + HP<sub>i</sub> [ $\Delta G_{\text{GA+HP}_i}^{\ddagger}$ ] is defined by the third-order rate constant  $k_{\text{cat}}/K_{\text{HP}_i}K_{\text{GA}}$  (Scheme 4). Figure 3 presents the linear logarithmic free energy correlation between the activation barriers for wild-type

Scheme 4

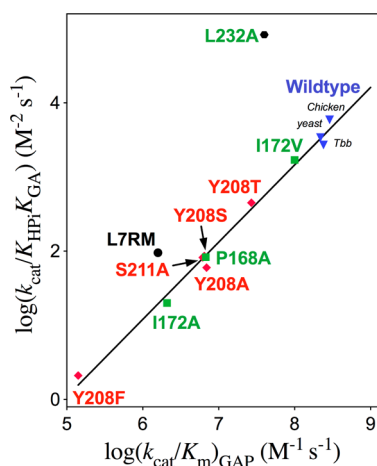
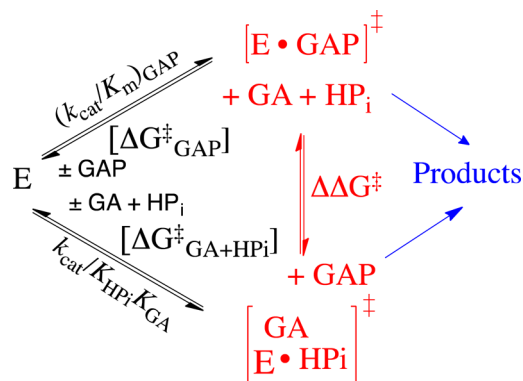


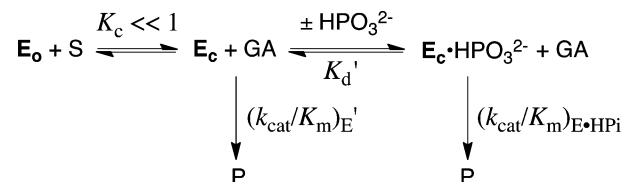
**Figure 3.** Linear free energy relationship, with slope  $1.04 \pm 0.03$ , between the second-order rate constant [ $\log(k_{\text{cat}}/K_{\text{m}})_{\text{GAP}}$ ] for wild-type and mutant TIM-catalyzed isomerization of GAP and the corresponding third-order rate constant [ $\log(k_{\text{cat}}/K_{\text{HPi}}K_{\text{GA}})$ ] for the enzyme-catalyzed reactions of the substrate pieces GA and  $\text{HPi}$ . Key: Green, *Tbb*TIM; black, *c*TIM; red, *y*TIM.

and mutant-TIM-catalyzed reactions of the whole substrate GAP and the substrate pieces GA +  $\text{HPi}$ . This correlation with slope of  $1.04 \pm 0.03$  (95% confidence interval; 0.97–1.11) shows that most of these mutations, which alter the interactions of ligands with flexible loops 6 and 7 (Figure 1),<sup>29</sup> result in the same destabilization of the transition states for the catalyzed reactions of the whole substrate and substrate pieces. We conclude that these transition states show strikingly similar interactions with TIM and that by this criteria are remarkably similar. The slope of 1.0 for Figure 3 reflects the constant difference in activation barriers for the reaction of whole substrate and the substrate in pieces:  $\Delta\Delta G^\ddagger = 6.6 \pm 0.3$  kcal/mol (Scheme 4). This difference is the entropic advantage to the binding of the transition state for the reaction of the whole substrate compared with the transition state for reaction of the two pieces.<sup>30</sup> This result is in good agreement with other estimates of the catalytic advantage obtained from covalent attachment of the reactants in a bimolecular reaction.<sup>31</sup>

The large positive deviation of the point for L232A mutant *Tbb*TIM from the correlation in Figure 3 reflects the 25-fold larger value of  $k_{\text{cat}}/K_{\text{HPi}}K_{\text{GA}}$  for the L232A mutant compared to wild-type TIM.<sup>17,18</sup> We have proposed that the L232A mutation results in a 25-fold increase in the equilibrium constant  $K_{\text{c}}$  for the thermodynamically unfavorable conversion of TIM from the

dominant inactive open form  $E_o$  to an active loop-closed form  $E_c$ , which is reflected by a  $\sim 25$ -fold increase in concentration of the active enzyme (Scheme 5).<sup>8,17,18</sup> We are uncertain of the

Scheme 5



explanation for the smaller positive deviation from this linear correlation of the kinetic parameters for the complex loop 7 replacement mutation of *c*TIM (Figure 3).

Wolfenden proposed that optimal enzymatic catalysis is sometimes obtained when the substrate is trapped in a protein cage, at an active site that provides for maximum enzyme–ligand contacts.<sup>32</sup> This catalytic cage is created when substrate or transition-state analogs bind to TIM, by the closure of a flexible gripper loop over the ligand phosphodianion<sup>22,26,33–35</sup> and presumably over the  $\text{HPi}$  activator. The linear correlation from Figure 3 provides evidence that dianions play a role as active spectators in creating the caged catalytic complex. The dianions are active and serve as a type of glue to hold TIM in a high-energy closed active form ( $E_c$ , Scheme 5), but in a different sense they are spectators, which provide no direct stabilization of the transition state for the unactivated reaction<sup>19</sup> and which do not affect the transition-state structure.

The results of previous studies on TIM and the decarboxylation catalyzed by orotidine 5'-monophosphate decarboxylase show that each enzyme is composed of a catalytic domain, which is competent to carry out the catalyzed reaction, and a dianion binding domain, where strong binding interactions with dianions are utilized to activate these enzymes for catalysis.<sup>36–38</sup> The present results provide evidence that interactions between TIM and a spectator dianion lock the enzyme into an active conformation that is otherwise present at low concentrations (Scheme 5). Part of the dianion binding energy is used to drive desolvation of the carboxylate side-chain of Glu-165 (*c*TIM and *y*TIM) or Glu-167 (*Tbb*TIM), which enhances the side-chain basicity toward deprotonation of carbon.<sup>27</sup> The dianion binding interactions might also be utilized to organize/position the catalytic side chains at the enzymatic transition state, consistent with the notion that there is a high degree of “preorganization” of these side chains at the active sites of efficient enzyme catalysts.<sup>39–41</sup>

## ■ ASSOCIATED CONTENT

### Supporting Information

Experimental procedures for the preparation and purification of Y208T, Y208S, Y208A, Y208F and S211A mutants of *y*TIM; procedures for determination of the product yields and kinetic parameters for wild-type and mutant *y*TIM-catalyzed reactions of [ $1\text{-}^{13}\text{C}$ ]-GA; Tables S1–S6, second-order rate constants and fractional product yields for the reaction of [ $1\text{-}^{13}\text{C}$ ]-GA catalyzed by wild-type *y*TIM (Table S1); and, by Y208T, Y208S, Y208A, Y208F and S211A mutants (Tables S2–S6, respectively); Table S7, kinetic parameters for wild-type and mutant *y*TIM-catalyzed reactions of GAP and of GA and  $\text{HPi}$ . This material is available free of charge via the Internet at <http://pubs.acs.org>.

## ■ AUTHOR INFORMATION

## Corresponding Author

jrichard@buffalo.edu

## Notes

The authors declare no competing financial interest.

## ■ ACKNOWLEDGMENTS

This work was supported by Grant GM39754 from the National Institutes of Health.

## ■ REFERENCES

- (1) Richard, J. P. *Biochemistry* **2012**, *51*, 2652.
- (2) Wierenga, R. K.; Kapetanious, E. G.; Venkatesan, R. *Cell. Mol. Life Sci.* **2010**, *67*, 3961.
- (3) Knowles, J. R. *Nature* **1991**, *350*, 121.
- (4) O'Donoghue, A. C.; Amyes, T. L.; Richard, J. P. *Biochemistry* **2005**, *44*, 2622.
- (5) Amyes, T. L.; O'Donoghue, A. C.; Richard, J. P. *J. Am. Chem. Soc.* **2001**, *123*, 11325.
- (6) Pompliano, D. L.; Peyman, A.; Knowles, J. R. *Biochemistry* **1990**, *29*, 3186.
- (7) Amyes, T. L.; Richard, J. P. *Biochemistry* **2007**, *46*, 5841.
- (8) Go, M. K.; Amyes, T. L.; Richard, J. P. *Biochemistry* **2009**, *48*, 5769.
- (9) Ray, W. J., Jr.; Long, J. W.; Owens, J. D. *Biochemistry* **1976**, *15*, 4006.
- (10) Kholodar, S. A.; Murkin, A. S. *Biochemistry* **2013**, *52*, 2302.
- (11) Goryanova, B.; Amyes, T. L.; Gerlt, J. A.; Richard, J. P. *J. Am. Chem. Soc.* **2011**, *133*, 6545.
- (12) Tsang, W.-Y.; Amyes, T. L.; Richard, J. P. *Biochemistry* **2008**, *47*, 4575.
- (13) Amyes, T. L.; Richard, J. P.; Tait, J. J. *J. Am. Chem. Soc.* **2005**, *127*, 15708.
- (14) Amyes, T. L.; Richard, J. P. *Biochemistry* **2013**, *52*, 2021.
- (15) Jencks, W. P. *Adv. Enzymol. Relat. Areas Mol. Biol.* **1975**, *43*, 219.
- (16) Morrow, J. R.; Amyes, T. L.; Richard, J. P. *Acc. Chem. Res.* **2008**, *41*, 539.
- (17) Malabanan, M. M.; Koudelka, A. P.; Amyes, T. L.; Richard, J. P. *J. Am. Chem. Soc.* **2012**, *134*, 10286.
- (18) Malabanan, M. M.; Amyes, T. L.; Richard, J. P. *J. Am. Chem. Soc.* **2011**, *133*, 16428.
- (19) Zhai, X.; Amyes, T. L.; Wierenga, R. K.; Loria, J. P.; Richard, J. P. *Biochemistry* **2013**, *52*, 5928.
- (20) Casteleijn, M. G.; Alahuhta, M.; Groebel, K.; El-Sayed, I.; Augustyns, K.; Lambeir, A.-M.; Neubauer, P.; Wierenga, R. K. *Biochemistry* **2006**, *45*, 15483.
- (21) Wang, Y.; Berlow, R. B.; Loria, J. P. *Biochemistry* **2009**, *48*, 4548.
- (22) Jögl, G.; Rozovsky, S.; McDermott, A. E.; Tong, L. *Proc. Natl. Acad. Sci. U.S.A.* **2003**, *100*, 50.
- (23) Sampson, N. S.; Knowles, J. R. *Biochemistry* **1992**, *31*, 8482.
- (24) Go, M. K.; Malabanan, M. M.; Amyes, T. L.; Richard, J. P. *Biochemistry* **2010**, *49*, 7704.
- (25) Go, M. K.; Koudelka, A.; Amyes, T. L.; Richard, J. P. *Biochemistry* **2010**, *49*, 5377.
- (26) Kursula, I.; Wierenga, R. K. *J. Biol. Chem.* **2003**, *278*, 9544.
- (27) Malabanan, M. M.; Nitsch-Velasquez, L.; Amyes, T. L.; Richard, J. P. *J. Am. Chem. Soc.* **2013**, *135*, 5978.
- (28) Donnini, S.; Groenhof, G.; Wierenga, R. K.; Juffer, A. H. *Proteins* **2006**, *64*, 700.
- (29) Malabanan, M. M.; Amyes, T. L.; Richard, J. P. *Cur. Opin. Struct. Biol.* **2010**, *20*, 702.
- (30) Page, M. I.; Jencks, W. P. *Proc. Nat. Acad. Sci. U.S.A.* **1971**, *68*, 1678.
- (31) Jencks, W. P. *Proc. Natl. Acad. Sci. U.S.A.* **1981**, *78*, 4046.
- (32) Wolfenden, R. *Mol. Cell. Biochem.* **1974**, *3*, 207.
- (33) Alahuhta, M.; Wierenga, R. K. *Proteins Struct., Funct., Bioinf.* **2010**, *78*, 1878.
- (34) Davenport, R. C.; Bash, P. A.; Seaton, B. A.; Karplus, M.; Petsko, G. A.; Ringe, D. *Biochemistry* **1991**, *30*, 5821.
- (35) Lolis, E.; Petsko, G. A. *Biochemistry* **1990**, *29*, 6619.
- (36) Spong, K.; Amyes, T. L.; Richard, J. P. *J. Am. Chem. Soc.* **2013**, *135*, 18343.
- (37) Goryanova, B.; Goldman, L. M.; Amyes, T. L.; Gerlt, J. A.; Richard, J. P. *Biochemistry* **2013**, *52*, 7500.
- (38) Amyes, T. L.; Ming, S. A.; Goldman, L. M.; Wood, B. M.; Desai, B. J.; Gerlt, J. A.; Richard, J. P. *Biochemistry* **2012**, *51*, 4630.
- (39) Warshel, A. *J. Biol. Chem.* **1998**, *273*, 27035.
- (40) Adamczyk, A. J.; Cao, J.; Kamerlin, S. C. L.; Warshel, A. *Proc. Nat. Acad. Sci. U.S.A.* **2011**, *108*, 14115.
- (41) Kamerlin, S. C. L.; Sharma, P. K.; Chu, Z. T.; Warshel, A. *Proc. Nat. Acad. Sci. U.S.A.* **2010**, *107*, 4075.